High-precision optical-frequency dissemination on branching optical-fiber networks

Sascha W. Schediwy,[1,*] David Gozzard,[1] Kenneth G. H. Baldwin,[2] Brian J. Orr,[3] R. Bruce Warrington,[4] Guido Aben,[5] and Andre N. Luiten[1,6]

[1]*School of Physics, University of Western Australia, WA 6009, Australia*

[2]*Research School of Physics and Engineering, The Australian National University, ACT 0200, Australia*

[3]*MQ Photonics Research Centre, Department of Physics and Astronomy, Macquarie University, NSW 2109, Australia*

[4]*National Measurement Institute, NSW 2070, Australia*

[5]*Australia's Academic and Research Network (AARNet), WA 6151, Australia*

[6]*Institute for Photonics and Advanced Sensing (IPAS) and School of Chemistry & Physics, The University of Adelaide, SA 5005, Australia*

**Corresponding author: sascha.schediwy@uwa.edu.au*

Received May 6, 2013; revised June 28, 2013; accepted July 10, 2013; posted July 11, 2013 (Doc. ID 189986); published July 31, 2013

We present a technique for the simultaneous dissemination of high-precision optical-frequency signals to multiple independent remote sites on a branching optical-fiber network. The technique corrects optical-fiber length fluctuations at the output of the link, rather than at the input as is conventional. As the transmitted optical signal remains unaltered until it reaches the remote site, it can be transmitted simultaneously to multiple remote sites on an arbitrarily complex branching network. This technique maintains the same servo-loop bandwidth limit as in conventional techniques and is compatible with active telecommunication links.

OCIS codes: (060.2360) Fiber optics links and subsystems; (120.3930) Metrological instrumentation; (120.5050) Phase measurement.

http://dx.doi.org/10.1364/OL.38.002893

Stabilization of optical-fiber links for the purpose of ultra-precise time and frequency transfer has seen a great deal of development since the early work of the 1990s [1,2]. Highlights include: optical-frequency transfers over a 920 km dark fiber link with a transfer stability of 5×10^{-15} at 1 s of integration [3]; microwave-frequency transfers over an 86 km urban link with a transfer stability of 1×10^{-15} at 1 s [4]; optical-frequency comb transfers over 7.7 km of dark fiber [5]; the simultaneous transfer of optical-frequencies and absolute time [6]; and the simultaneous transfer of optical and microwave-frequencies alongside digital data on telecommunication links [7]. However, all of these techniques can only provide stabilized signals to a single remote site.

Recently, an extension was proposed that can provide stabilized optical-frequency signals at intermediate sites along a length of optical fiber [8], and the technique was amended to also demonstrate the transfer of microwave-frequencies at intermediate sites [9]. However, as the intermediate sites rely on mixing signals received from the source and from the far end of the fiber, this approach is limited to fiber links with a linear topology.

By contrast, many applications require the transfer of signals from a single master site to multiple remote sites over a fiber network with a branching topology; these include connected-element interferometer radio telescopes like the planned Square Kilometre Array [10], research campuses, and metropolitan networks. As shown in Fig. 1(A), such a network can be broken into multiple, daisy-chained, individually-stabilized linear segments. However, this implementation has two drawbacks: (1) if the stabilization servo of one segment fails, then the transfer to all downstream remote sites ceases to be stabilized and (2) additional stabilized nodes need to be installed, so in this example, transfer to five locations requires eight independent link stabilization servos. The implementation shown in Fig. 1(B) requires no additional intermediate stabilized nodes, so that transfer to each remote site is simultaneous and independent. This has the advantage that if a single stabilization servo fails then only a single remote site will lose its stable signal. In this Letter we describe a technique that delivers this simultaneous and independent transfer to each remote node.

A schematic of this technique is illustrated in Fig. 2. An optical-frequency ν_0 is sent from the Signal Source along a fiber link to a remote site (we use Remote A as an example, but the same applies to any remote site). Temporal variations of a link's optical path length L_{opt} resulting from vibrations and temperature changes, bring about

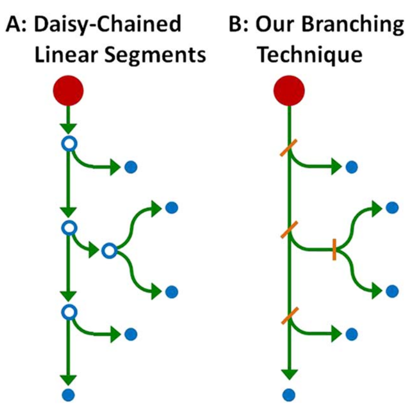

Fig. 1. Example of an optical-fiber network showing the different implementations required to provide stabilized signals to five remote sites: A, conventional techniques applied to stabilize daisy-chained, individual linear segments; B, our branching stabilization technique.

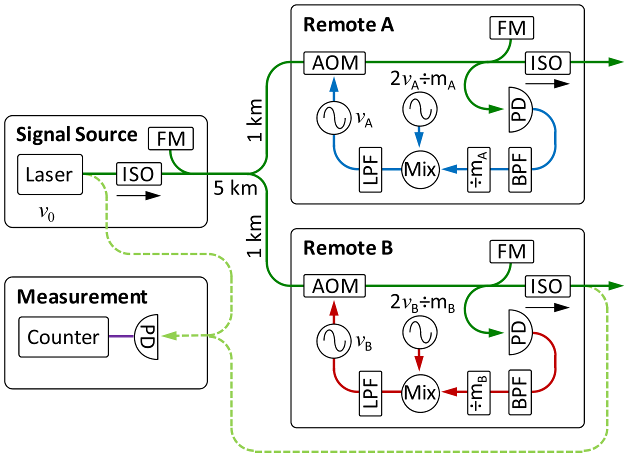

Fig. 2. Schematic diagram of our branching optical-fiber stabilization technique. $\nu_0 = 193$ THz; $\nu_A = 40$ MHz; $m_A = 10$; $\nu_B = 70$ MHz; $m_B = 17$; ISO, optical isolator; FM, Faraday mirror; AOM, acousto-optic modulator; PD, photodetector; LPF, low-pass filter; BPF, bandpass filter; $\div m$, frequency divider; Mix, mixer.

variations of the refractive index and physical length of the link. This causes frequency changes $\Delta\nu_{\text{Link-A}}$ of a signal transported through this link, given by

$$\Delta\nu_{\text{Link-A}} = \frac{\nu_0}{c_0}\frac{d}{dt}L_{\text{opt}}(t), \tag{1}$$

where c_0 is the speed of light in vacuum. At Remote A, the optical signal passes through an acousto-optic modulator (AOM) that imparts a frequency shift ν_A. Therefore, the optical signal after the AOM can be expressed as

$$\nu_{A,1} = \nu_0 + \nu_A + \Delta\nu_{\text{Link-A}}. \tag{2}$$

Part of the frequency-shifted signal is reflected by a Faraday mirror (FM) and a fraction of the power is directed to a photodetector (PD), while the remainder returns to the source site through the AOM and fiber link for a second time. At the source site, the signal is now: $\nu_{A,2} = \nu_0 + 2\nu_A + 2\Delta\nu_{\text{Link-A}}$. Part of this signal is reflected by a second FM and is transmitted along the link and through the AOM for a third time ($\nu_{A,3} = \nu_0 + 3\nu_A + 3\Delta\nu_{\text{Link-A}}$). The PD at Remote A detects the mixing product between $\nu_{A,1}$ and $\nu_{A,3}$. The PD's output is bandpass-filtered (BPF) at a center frequency $2\nu_A$ to isolate the frequency difference between $\nu_{A,1}$ and $\nu_{A,3}$, mixed with a local oscillator at $2\nu_A$, and low-pass filtered to give

$$S_{\text{Mix}} = \nu_{A,3} - \nu_{A,1} - 2\nu_A = 2\Delta\nu_{\text{Link-A}}. \tag{3}$$

S_{Mix} is then used at Remote A to modulate the frequency of its AOM drive signal. This action closes the servo loop to stabilize the optical length of the link in the same way as with conventional optical-stabilization techniques [2]. S_{Mix} is a beat signal between the first and third passes of the link which are, as in conventional stabilization, separated in time by one round trip through the fiber link. We thus have the same bandwidth limitations with this new system as in the conventional systems [2]. Multiple reflections between the two FMs produce higher-order contributions to $2\nu_A$; however, in practical implementations, the magnitude of these will decrease by around 20–40 dB for each additional pass of the link owing to the additional optical losses from the FM splitters.

With the stabilization servo engaged, the AOM adds an identical correction $\Delta\nu_A$ to all three optical signals that pass through it. The resultant signals, $\nu'_{A,1}$, $\nu'_{A,3}$, and $\nu'_{A,3}$, are denoted by the addition of a prime. Engaging the stabilization servo has the effect of driving S'_{Mix} to zero

$$S'_{\text{Mix}} = \nu'_{A,3} - \nu'_{A,1} - 2\nu_A \approx 0. \tag{4}$$

The magnitude of $\Delta\nu_A$ is therefore such that it cancels the fluctuations induced from a single pass of the link

$$\Delta\nu_A \approx -\Delta\nu_{\text{Link-A}}. \tag{5}$$

This dictates that the AOM also applies the appropriate correction to suppress fluctuations of $\nu_{A,1}$ as shown:

$$\nu'_{A,1} = \nu_0 + \nu_A + \Delta\nu_{\text{Link-A}} + \Delta\nu_A \approx \nu_0 + \nu_A. \tag{6}$$

We repeat that, in contrast to conventional techniques, the correction to suppress fiber-length fluctuations is implemented at the output of the link rather than at the input. This has the advantage that the transmitted optical signal ν_0 remains unaltered until it reaches the remote site; therefore, ν_0 can be transmitted simultaneously to multiple remote sites. This enables establishment of time- and frequency-transfer networks that can be branched multiple times at arbitrary positions along optical-fiber links, such shown in Fig. 1(B).

A key element of the branching technique is that each remote site requires a unique AOM frequency to distinguish it from the AOM frequencies used by the other remote sites. Furthermore, the harmonics generated by multiple passes of the link must also not overlap with any signals generated at other sites. Nonetheless, we calculate that it is practicable to realize a network with dozens or even hundreds of independent sites, separated from each other in frequency by more than the desired control-loop bandwidth (perhaps 1 MHz), while all signals remain within a single telecommunication channel (100 GHz). A practical drawback, relative to the conventional link-stabilization techniques, is the additional optical loss due to the power splitters used to construct the branching network. However, this can be overcome by including additional bidirectional optical amplifiers [11]. In practical deployment over links where the optical loss due to fiber attenuation is balanced by the gain of in-line optical amplifiers, the requirement for an extra signal pass by this technique does not necessitate the use of any additional amplifiers.

We have demonstrated this technique by using the simplest configuration that possesses all the critical elements of a branching topology, namely, the two-way branching topology shown in Fig. 2. A Grade 4 RIO PLANEX laser (spectral linewidth <3 kHz), situated at the Signal Source, and operating at a wavelength of 1552 nm ($\nu_0 = 193$ THz), was used to transmit an optical-frequency signal along a 5 km spool of fiber. The signal was then split equally into two parts, each part

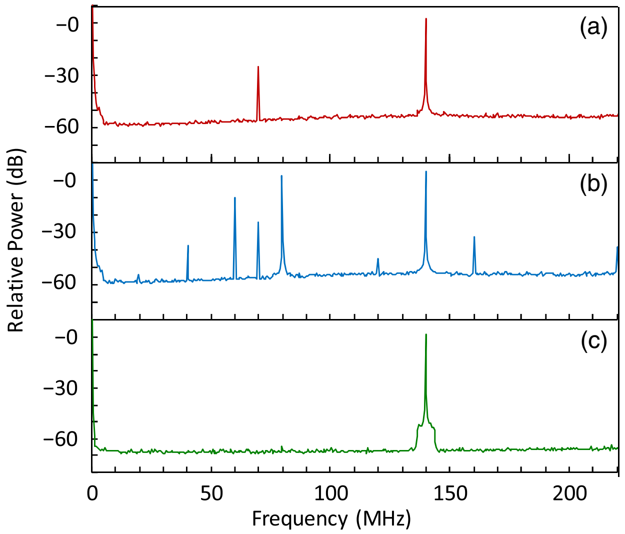

Fig. 3. Normalized power spectrum as measured by the PD at Remote B: A, with Remote A disconnected; B, with Remote A connected; C, with Remote A connected but after a bandpass filter centered on 140 MHz.

being transmitted along a further 1 km section of spooled fiber to two remote sites: Remote A and Remote B. All optical splitters had a splitting ratio of 50%. This preliminary demonstration was over relatively short fiber lengths, but the technique is equally applicable to longer fiber given a laser with a narrower linewidth.

The AOM frequencies at the two remote sites were: $\nu_A = 40$ MHz and $\nu_B = 70$ MHz. Figure 3 shows the power spectrum measured by the PD at Remote B under the following conditions: A, with Remote A disconnected; B, with Remote A connected; and C, as in B, but after a bandpass filter centered on 140 MHz, which suppresses all unwanted signals by at least 60 dB below the signal of interest. The unwanted signals are further rejected in the mixing process and by a low-pass filter at the output of the mixer. The link-stabilization servos were engaged by activating the frequency modulation function on each site's AOM source. Frequency division was used to help achieve a stable servo lock; the division factors of $m_A = 10$ for Remote A and $m_B = 17$ for Remote B were chosen so that the resulting output frequencies matched available filters.

Both remote sites were co-located within the same laboratory as the signal source, permitting an independent measure of the transfer stability to each site using the "Measurement" section of the experiment shown in Fig. 2. The out-of-loop fiber connections (dashed lines) were kept as short as practicable and were thermally and acoustically isolated. The estimated fractional frequency stabilities of the optical-frequency transfer, as measured by a Λ-type frequency counter, are plotted as a function of integration time in Fig. 4.

The traces in panel A were measured at Remote A and traces in panel B were measured at Remote B. For the plots in each panel, dashed lines with filled markers indicate the transfer fractional frequency stability between the source and each remote site when the link length was uncontrolled (3.1×10^{-14} at 1 s for Remote A and 2.0×10^{-14} at 1 s for Remote B), while solid lines with filled

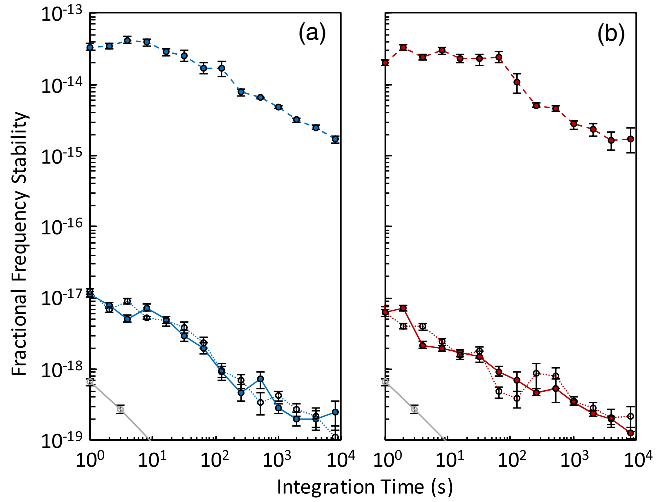

Fig. 4. Fractional frequency stability of optical-frequency transfer measured separately at Remote A (panel A) and Remote B (panel B): with the stabilization servo disengaged (dashed lines, filled markers), with the stabilization servo engaged while the other site is disconnected (dotted lines, open markers), and while connected (solid lines, filled markers); frequency-counter noise floor (solid lines, open markers).

markers show the transfer stability to each remote site with both servos operating simultaneously (1.2×10^{-17} at 1 s for Remote A and 6.4×10^{-18} at 1 s for Remote B). Finally, dotted lines with open markers show the transfer stability to each remote site with the relevant stabilization servo engaged but with the other branch physically disconnected (1.1×10^{-17} at 1 s for Remote A and 6.2×10^{-18} at 1 s for Remote B). We conclude that the inclusion of the extra site has no impact on the transfer stability, given that the transfer-stability data fall within the uncertainty across the entire range of integration times for each site. Moreover, the accuracy of the frequency transfer is not affected by the inclusion of the extra site: in the case of Remote A, the average transfer accuracy over the range of integration times was $(2.0 \pm 1.1) \times 10^{-18}$ while both servos were operating simultaneously, and $(3.4 \pm 1.8) \times 10^{-18}$ when Remote B was physically disconnected.

We have demonstrated high-precision, simultaneous transfer of optical-frequency signals to multiple locations. This technique can be expanded onto an arbitrarily complex branching network. Such a system obviates the need for additional intermediate stabilization equipment, and is robust to the failure of other stabilized links in the network, when compared to the daisy-chained linear alternative. Moreover, our technique has the same servo-loop bandwidth limits as conventional techniques, and can be deployed across active telecommunication links.

This work was supported by the Australian Research Council's Linkage Projects (LP110100270) and Future Fellowship (FT0991631) funding schemes.

References

1. T. P. Krisher, L. Maleki, G. F. Lutes, L. E. Primas, R. T. Logan, J. D. Anderson, and C. M. Will, Phys. Rev. D **42**, 731 (1990).

2. L.-S. Ma, P. Jungner, J. Ye, and J. L. Hall, Opt. Lett. **19**, 1777 (1994).
3. K. Predehl, G. Grosche, S. M. F. Raupach, S. Droste, O. Terra, J. Alnis, T. Legero, T. W. Hänsch, T. Udem, R. Holzwarth, and H. Schnatz, Science **336**, 441 (2012).
4. O. Lopez, A. Amy-Klein, M. Lours, C. Chardonnet, and G. Santarelli, Appl. Phys. B **98**, 723 (2010).
5. G. Marra, H. S. Margolis, and D. J. Richardson, Opt. Express **20**, 1775 (2012).
6. O. Lopez, A. Kanj, P.-E. Pottie, D. Rovera, J. Achkar, C. Chardonnet, A. Amy-Klein, and G. Santarelli, Appl. Phys. B **110**, 3 (2013).
7. S. Schediwy, A. Luiten, G. Aben, K. Baldwin, Y. He, B. Orr, and B. Warrington, in *Proceedings of the 2012 EFTF* (2012), p. 211.
8. G. Grosche, "Verfahren zum Bereitstellen einer Referenz-Frequenz," DPMA Patent application DE 102,008,062,139 (June 24, 2010).
9. C. Gao, B. Wang, W. L. Chen, Y. Bai, J. Miao, X. Zhu, T. C. Li, and L. J. Wang, Opt. Lett. **37**, 4690 (2012).
10. P. E. Dewdney, P. J. Hall, R. T. Schilizzi, and T. J. L. W. Lazio, Proc. IEEE **97**, 1482 (2009).
11. N. R. Newbury, P. A. Williams, and W. C. Swann, Opt. Lett. **32**, 3056 (2007).